Trade-off between virulence and dispersal drives parasite evolution at experimental invasion front

Louise Solveig Nørgaard[1,2#*], Giacomo Zilio[2#], Camille Saade[2], Claire Gougat-Barbera[2], Matthew D. Hall[1], Emanuel A. Fronhofer[2] & Oliver Kaltz[2*]

[1]School of Biological Sciences and Centre for Geometric Biology, Monash University, Melbourne 3800, Australia

[2]ISEM, University of Montpellier, CNRS, EPHE, IRD, Montpellier, France.

*Corresponding author: oliver.kaltz@umontpellier.fr; louise.noergaard@monash.edu

[#]Shared first author contribution

Keywords: *Paramecia caudatum*, *Holospora undulata*, host-parasite interactions, experimental evolution, disease, evolution, trade-off, virulence

ABSTRACT

Understanding the occurrence and spatial spread of infectious disease is a major challenge to epidemiologists and evolutionary biologists. Current theory predicts the spread of highly exploitative parasites at the front of spreading epidemics. However, many parasites rely on the dispersal of their hosts to spread to new habitats. This may lead to a conflict between local transmission and spatial spread, counteracting selection for highly virulent parasites. Yet, there are no experimental tests of these hypotheses. Here we investigate parasite evolution in an experiment creating conditions in cores and at fronts of spreading host-parasite populations, using the freshwater host *Paramecium caudatum* and its bacterial parasite *Holospora undulata.* We find that parasites from experimental range fronts induce higher rates of host dispersal than parasites from the core. This divergence is accompanied by lower levels of virulence and delayed development of infectious stages of front parasites. We validate these experimental results by fitting an epidemiological model to time-series data independently obtained from the experiment. This combined evidence suggests an evolutionary trade-off between host exploitation (virulence) and host-mediated dispersal, resulting in a shift of the investment in horizontal transmission. In conclusion, our results show that different segments of an epidemic wave may be under divergent selection pressures, shaping the evolution of parasite life history. These findings have important implications for our understanding of the interaction between demography and rapid evolutionary change in spreading populations, which is crucial for the management of emerging diseases, biological invasions and other non-equilibrium scenarios.

INTRODUCTION

Epidemic outbreaks of infectious disease are of great concern to human health, agriculture and wildlife conservation, and understanding the ecological and evolutionary drivers of their spread represents a major challenge to epidemiologists and evolutionary biologists (Parratt et al., 2016; Penczykowski et al., 2016). In spatially homogeneous populations, theory often predicts the spread of highly exploitative (i.e., virulent) parasites with a high transmission potential (Andre and Hochberg, 2005). Outbreaks of disease in the wild, however, generally occur in highly dynamic or patchy host populations, such as in metapopulations or in range expanding and invasive species. Since many parasites spread to new habitats via host-mediated dispersal, the evolution of such parasites will now depend not only on the strategies that maximise transmission in response to changes in host demography (Nørgaard et al., 2019a; Penczykowski et al., 2016), but also on a correlated response to the spatial sorting of hosts with different dispersal capacities across a landscape (see (Calcagno et al., 2006; Perkins et al., 2013). However, how the increased mobility of a host during range expansion processes (Phillips et al., 2010) translates into the emergence and spread of infectious disease, remains unclear due to the high complexity of ecological and evolutionary dynamics at play (see (Dunn and Hatcher, 2015; Perkins et al., 2008; Torchin et al., 2003).

By exploring the many different levels of virulence in nature, Ewald (1995) suggested that parasite transmission and virulence may evolve in response to changes in the opportunity for dispersal provided by a particular vector, such as the recurrent emergence of highly virulent cholera strains during periods with high water supply and low purification. Other studies have also established that moving parasites are likely to evolve ‘invasion syndromes’, with characteristic transmission strategies and dispersal behaviours, such as increased size of transmission propagules, and allowing for higher host-facilitated dispersal (Berngruber et al., 2013; Kelehear et al., 2012; Phillips and Puschendorf, 2013). Empirical support for such

predictions has subsequently emerged, and show the emergence of highly virulent honeybee viruses (Mondet et al., 2014) and rabbit haemorrhagic disease virus (Boots et al., 2004; Moss et al., 2002) at the front of a progressing epidemic. Yet, not all host-parasite systems necessarily show this pattern. For instance, the geographic spread of the bacterium *Mycoplasma gallisepticum* in North American house finches was associated with decreased virulence in the newly invaded areas (Hawley et al., 2013). Likewise, in monarch butterflies, hosts that sustain long or frequent migrations are infected with less virulent parasites (de Roode et al., 2008).

Recent theory has begun to develop a conceptual framework to investigate parasite evolution in spatially explicit, non-equilibrium settings. Assuming a classic virulence-transmission trade-off (Bull, 1994; Gandon et al., 2001; May and Anderson, 1983) and local feedbacks between epidemiology and selection, several models predict that more virulent parasites will evolve in highly connected "small-world" landscapes (Boots et al., 2004; Kamo and Boots, 2006; Kamo et al., 2007), or at the front of an advancing epidemic (Griette et al., 2015), where host exploitation and transmission is not limited by local depletion of susceptible hosts (“self-shading”). In contrast, a more explicit consideration of hosts dispersal can lead to a different prediction (Osnas et al., 2015; Nørgaard et al., 2019a). If parasites travel with their infected hosts, exploitation of host resources may reduce dispersal, thereby introducing a novel dispersal-virulence trade-off. Thus, Osnas et al (2015) show that selection at the moving edge favours more prudent and dispersal-friendly parasites that escape more virulent and transmissible parasites from the core of an epidemic (Osnas et al., 2015). This latter idea mirrors classic principles from metapopulation theory and metacommunity ecology, based on trade-offs between competitive ability and colonisation/dispersal (Calcagno et al., 2006;Olivieri et al, 1995).

With a growing number of range expanding (Epstein, 2000), invasive (Dunn and Hatcher, 2015), or colonising host populations (Thomas, 2000), there has been increasing

interest in what types of parasite 'invasion syndromes' might emerge at the front of expanding host populations (Dunn and Hatcher, 2015). However, while the study of parasites from natural invasion fronts provides valuable information, controlled empirical investigations remain rare. Experimental approaches test how population 'viscosity' (and therefore local vs. global dispersal) impacts on disease evolution (Boots and Mealor, 2007; Kerr et al., 2006; Vogwill et al 2010) or manipulate demographic conditions to mimic the front and core of an expanding epidemic (Nørgaard et al., 2019a). To our knowledge, so far, no studies have addressed parasite evolution under natural dispersal, or the evolution of parasite dispersal itself.

Experimental evolution in experimental microcosm populations provides a powerful tool to test hypotheses about parasite evolution under controlled conditions for a large number of generations (Brockhurst and Koskella, 2013). Moreover, for organisms with directed movement, experimental landscapes can be created to study metapopulation processes or range expansion dynamics (Friedenberg 2003; Fronhofer and Altermatt, 2015; Williams et al. 2016 flour beetle work). Here, we investigated the experimental evolution of spatially spreading parasites, where all parasite dispersal is host-mediated. Using two-patch dispersal arenas for the ciliate *Paramecium caudatum* and the bacterial parasite *Holospora undulata*, we mimicked a range expansion scenario, with a front population of hosts constantly dispersing naturally into a new microcosm, and a core population constantly remaining in place (and losing emigrants).. After 56 episodes of dispersal selection, we assayed evolved front and core parasites under common garden conditions and compared them for multiple traits, namely their effects on host dispersal, investment in horizontal transmission and virulence.

Because parasite persistence in the front populations depended entirely on host dispersal, we predicted front parasites to evolve minimal impact on host dispersal (Fellous et al 2011), or to even increase dispersal of infected hosts (Lion et al., 2006). Following Osnas *et al.* (2015), this could be achieved by reducing virulence, thereby generating an evolutionary

trade-off with investment in transmission capacity, not expected to occur in the core populations. The results from our assay were broadly consistent with predictions and validated by a simple epidemiological model fitted on an independent data set. We conclude that selection pressures at core and front of an invasion can lead to marked divergence of important parasite life-history traits and lead to the emergence of a 'parasite dispersal syndrome'.

MATERIALS AND METHODS

Study system

Paramecium caudatum is a filter-feeding freshwater protozoan ciliate from still water bodies in the Northern Hemisphere (Wichterman, 1986). It has a germline micronucleus and a somatic macronucleus. Our cultures are maintained asexually in a lettuce medium with the food bacterium *Serratia marcescen*s at 23 °C, allowing 1-2 population doublings per day (Nidelet and Kaltz, 2007).

The gram-negative alpha-proteobacterium *Holospora undulata* infects the micronucleus of *P. caudatum*, and can be transmitted both horizontally (by s-shaped infectious forms, 15µm) upon host death or during cell division, and vertically, when reproductive bacterial forms (5µm) segregate into daughter nuclei of a mitotically dividing host (Görtz and Dieckmann, 1980). After ingestion by feeding *Paramecium*, infectious forms invade the micronucleus, where they differentiate into the multiplying reproductive forms. After 1 week, reproductive forms begin to differentiate into infectious forms (Fels et al., 2008; Nidelet and Kaltz, 2007). Infectious hosts (i.e., producing the s-shaped transmission stages) can be easily identified under a contrast phase microscope (1000x magnification). Infection with *H. undulata* reduces host cell division and survival (Restif and Kaltz, 2006) and also host dispersal (Fellous et al., 2011).

Long-term experiment

Similar to Fronhofer and Altermatt (2015), we imposed dispersal selection in 2-patch microcosm arenas (SI 1, Fig. S1), built from two 14-mL plastic tubes, interconnected by 5-cm silicon tubing, which can be blocked or opened with a clamp. We define dispersal as the active swimming of *Paramecium* from one microcosm to the other via the connection tubing (i.e., the dispersal corridor).

The experiment was seeded from an uninfected host line ("63D", haplotype b05) from our laboratory that had been under "core selection" (see below) for three years and shows characteristically low dispersal propensity (O.K., unpublished data). A 63D mass culture was infected with an inoculum of *H. undulata* prepared from a mix of various infected stock cultures (for extraction protocol, see Supplementary Information S2). All parasites in this mix originate from a single isolate of *H. undulata* brought into the lab in 2001.

In the front selection treatment, we placed infected *Paramecium* in one tube ("core patch") and opened the connection for three hours, allowing them to swim into the second tube ("front patch"). *Paramecium* from the front patch were recovered and cultured in bacterised medium, allowing free host population growth and parasite transmission. After one week, we imposed another dispersal episode, again recovering only the *Paramecium* from the front patch, and so on. The core selection treatment followed the same alternation of dispersal episodes and growth periods, except that only *Paramecium* from the core patch were recovered and propagated (SI 1, Fig. S2). We established 5 'core selection' lines and 5 'front selection' lines that were maintained for a total of 56 episodes of dispersal. To minimise potential effects of host (co)evolution, we extracted infectious forms from each selection line after cycle 30, inoculated a new batch of naïve, 63D hosts and continued the experiment for the remaining 26 cycles. For details of the experimental protocols, see Supplementary Information (section S1 and S3).

Measurements. During the long-term experiment, we took routine measurements of population density, infection prevalences and dispersal rate (see Supplementary Information SI 3, Fig. S3). Densities were estimated by counting the number of cells in small samples (0.2-1 ml) under a dissecting microscope. To estimate infection prevalence in a population, ≈20 arbitrarily picked individuals were placed on a microscope slide and stained with 1% lacto-aceto orcein (Fokin and Görtz, 2009). Under a microscope (phase-contrast, 1000x magnification), we determined the proportion of infected hosts (absence/presence of infection) and the stage of infection, namely whether the parasite was producing horizontal transmission stages (infectious forms). Such hosts were considered 'infectious' (see Nidelet et al. 2007).

Parasite assays

At the end of the experiment, we extracted parasites from core and front selection lines to inoculate new, naïve hosts. We then assayed parasite effects on host dispersal, infection life-history and virulence. To assess the generality of trait expression, we tested the evolved parasites on naïve 63D hosts, but also on two other genotypes, C023 and C173 (provided by S. Krenek, TU Dresden, Germany). Companion assays of long-term host change are reported elsewhere (Zilio et al., 2020)).

All assays were performed on a cohort of infected replicate cultures, over the course of 3 weeks under common-garden conditions. To initiate the cultures, we placed ≈ 5 x 10^3 cells of a given naïve host genotype in 1.4 ml of bacterised medium in a 15ml tube, to which we added the freshly prepared inoculum of a given evolved parasite line (≈ 1.5 x 10^6 infectious spores, on average). On day 4 post-inoculation (p.i.), when most infections have established, we split the cultures into 3 technical replicates and expanded the volume to 30 ml, by adding bacterised medium. In total, we set up 90 replicate cultures (2 selection treatments x 5 parasite selection

lines x 3 host genotypes 3 technical replicates). We also prepared additional uninfected replicate cultures from each host genotype (exposed to a 'mock inoculum' prepared from uninfected cultures), which were used as a benchmark reference in certain assays.

Dispersal of infected hosts

Between day 14 and 19 p.i., we assayed the dispersal rates of hosts infected with core and front parasites. We used linear 3-patch arenas (SI 4, Fig. S4), where the *Paramecium* disperse from the middle tube to the two outer tubes, thereby yielding larger number of dispersers than 2-patch systems. Arenas were filled with ~2800 individuals in the middle tube. After 3 h of free dispersal, we took samples from the middle tube (0.5 mL) and from the pooled two outer tubes (3 mL) to estimate the number of non-dispersers and dispersers in the tubes. From LAO fixations (see above), we further determined the proportion of infected dispersers and non-dispersers, and then calculated the dispersal rate of infected hosts (number of dispersed infected hosts / total number of infected hosts per 3 h). Each of 88 available replicate cultures was tested once. For statistical analysis, we excluded 13 replicates with very low population density and/or infection prevalence (<10%), which prevented accurate estimation of dispersal of infected individuals. Dispersal was not significantly affected by assay date ($\chi_2^2 = 2.56$, $p > 0.25$), and this factor was therefore omitted from further analysis.

Parasite life-history traits

<u>Infectivity</u>. On day 4 p.i., we estimated infection prevalence in the initial 30 inoculated cultures, using LAO fixation. This measurement describes 'parasite infectivity', i.e., the capacity to successfully establish infections (Fels et al., 2008).

Epidemiology and parasite development (latency). From day 6 to 13 p.i., we tracked population density and infection prevalence in the 90 replicate cultures, using a blocked sliding window (day 6-8, 11-13) and ensuring that each parasite x host combination was measured once per day. These data were used for the fitting of an epidemiological model (see below). For day 6 to 11 p.i., we further recorded the proportion of infectious hosts in LAO-fixed samples. These series of 'snapshots' describe the timing and level of investment into horizontal transmission by the first cohort of the parasite (Nidelet et al 2007).

Virulence. To assess parasite effects on host fitness (virulence), we isolated single infected individuals from the replicate cultures on day 5 p.i., and allowed them to multiply in 2-mL plastic tubes with bacterised medium, under permissive common-garden conditions. After verifying infection status of these monoclonal cultures (LAO fixation), we started the virulence assay by placing single individuals in PCR tubes filled with 200 µL of medium. We checked tubes daily for absence or presence of cells for 20 days. In addition, cell density was determined on day 2 and 3 (by counting cells through the plastic tubes), on day 10 (from 50-µL samples) and on day 20 (total volume). Except for 50 µl of medium added on day 10, no resources were supplied. The assay was performed for 28 of the 30 combinations of parasite selection line and host genotype, with 8-12 infected singletons tested per combination, giving a total of 322 replicates. Of these, 17 died within less than 24 h (possibly due to transfer handling) and were excluded from statistical analysis testing for variation in cell number (day 2, 3, 10, 20) and replicate survival. In parallel, we prepared and assayed uninfected singletons, which served as supplementary reference points.

Statistical analysis

All statistical analyses were performed in R (ver. 3.3.3; R Development Core Team, available at www.r-project.org). To analyse variation in parasite traits, we used generalised linear mixed-effect models. Binomial error structure and logit link were used for analysis of infected host dispersal (proportion dispersers), infectivity (proportion infected individuals on day 4 p.i.), latency (proportion infectious hosts day 6-11 p.i.) and replicate survival in the virulence assay (proportion of replicates alive after 20 days). Poisson error structure and log link were used for analysis of cell number (day 2-20) in the virulence assay. Parasite selection treatment (front vs core) was taken as a fixed effect, host genotype and selection line identity as random factors. Time was integrated as a covariate in the latency analysis, and as a fixed factor in the virulence analysis. The significance of fixed effects was tested using analysis of variance (ANOVA Type III, car package: Fox & Weisberg, 2018).

Fitting an epidemiological model to time series data

We fitted a simple epidemiological model to the above population density and infection prevalence data recorded for our assay replicate cultures (day 6-13 p.i.). The aim was to obtain additional independent estimates of parasite parameters (Table 1), namely virulence, but also the transmission parameter or latency time, i.e. the time to onset of production of infectious forms (Rosenbaum et al., 2019).

Model structure. We model the density of non-infected (S) and infected (I) species using ordinary differential equations (ODEs). In the absence of parasites, we consider that non-infected *Paramecium* growth follows the continuous time version of the Beverton-Holt model (Thieme 2018).

$$\frac{dS}{dT} = \left(\frac{b}{1+\alpha N} - d\right) S \quad (1)$$

where b is a birth rate, d a death rate and α a competition term. N is the total number of individuals (S +I), which is equal to S here.

In the presence of infected individuals, uninfected individuals become infected at a rate proportional to the number of infected and non-infected individuals at a rate β:

$$\frac{dS}{dT} = \left(\frac{b}{1+\alpha N} - d\right) S - \beta SI \quad (2)$$

$$\frac{dI}{dT} = \beta SI \quad (3)$$

Moreover, infected individuals also display Beverton-Holt dynamics, but their birth rate can be decreased, hence we multiply b by a term $(1 - v)$, where v is the virulence of the parasite:

$$\frac{dS}{dT} = \left(\frac{b}{1+\alpha N} - d\right) S + \beta SI \quad (4)$$

$$\frac{dI}{dT} = \left(\frac{b(1-v)}{1+\alpha N} - d\right) I + \beta SI \quad (5)$$

Finally, vertical transmission of the parasite is not necessarily 100%, and some of the *Paramecium* "born" from infected individuals could be free of parasites. We name γ the proportion of successful vertical transmission:

$$\frac{dS}{dT} = \left(\frac{b}{1+\alpha N} - d\right) S - \beta SI + \left(\frac{b(1-v)}{1+\alpha N}\gamma\right) I \quad (6)$$

$$\frac{dI}{dT} = \left(\frac{b(1-v)}{1+\alpha N}\gamma - d\right) I + \beta SI \quad (7)$$

Since the majority of infected individuals were not yet producing infectious forms at the beginning of the time series, we added another parameter, τ, which is the latency before an infected individual becomes infectious (i.e., capable of horizontal transmission):

$$\beta = 0 if time < \tau \quad (8)$$

Table 1. Model parameters, their signification and the priors used for fitting.

Parameters	Meaning	Priors
b	Birth rate	Posteriors from fitting eq. (1) on non-infected population data
d	Death rate	
α	Intraspecific competition coefficient	
ν	Virulence (decrease in b)	Uniform(0, 1)
β	Horizontal transmission rate	Lognormal(-5, 0.9)
γ	Vertical transmission rate	Uniform(0.5, 1)
τ	Latency time	Uniform(144, 240)

Model Fitting. We fitted the epidemiological model to the data, using Bayesian inference and the *rstan* R package (version 2.19.2). Using data from previous experiments (O. Kaltz, unpublished data), we first fitted the Beverton-Holt model (Eq. 1) to growth curves of uninfected populations to estimate the distributions of *b, d* and *α* for each host genotype. These distributions were used as priors for fitting the full model (Eq. 6, 7, 8) on infection data. The model was fitted separately for each of the 6 combinations of host genotype and parasite selection treatment. For simplicity, we fitted a single set of parameters (*b, d, α, b, β, γ, τ*) over the different selection lines (with different initial conditions fitted over each line). Priors distributions can be found in Table 1. Apart from *b,* d and α, we used lowly informative priors that largely encompass expected values (*ν* and *γ* priors are uniform over possible values, *τ* prior is uniform over previously observed latency values, *β* prior follows a lognormal distribution an

order of magnitude wider than expected values). Fits were realized using the No U-Turn Sampler (NUTS) with default rstan values and multiple chains (3 chains per fit, each of total length: 15 000 and warm-up length = 5 000).

RESULTS

Infected host dispersal

On average, hosts infected with front parasites tended to disperse more than those infected with the core parasites (24 % vs 12 %; Fig. 1). This effect was marginally significant (χ_1^2 =4.20, p = 0.0403), with considerable scatter of observed values in both groups. Nonetheless, the trend was consistent on all three host genotypes, with on average 7 to 20% higher dispersal of front parasites (SI 5, Fig. S5). Furthermore, the observed patterns were robust to variation in demographic or epidemiological conditions, as neither population density nor infection prevalence in the replicate cultures had significant effects on dispersal rates when added to our statistical model ($p > 0.25$; details not shown). Overall, dispersal rates of infected hosts were lower than those generally observed in uninfected cultures of the three host genotypes (SI 5, Fig. S5).

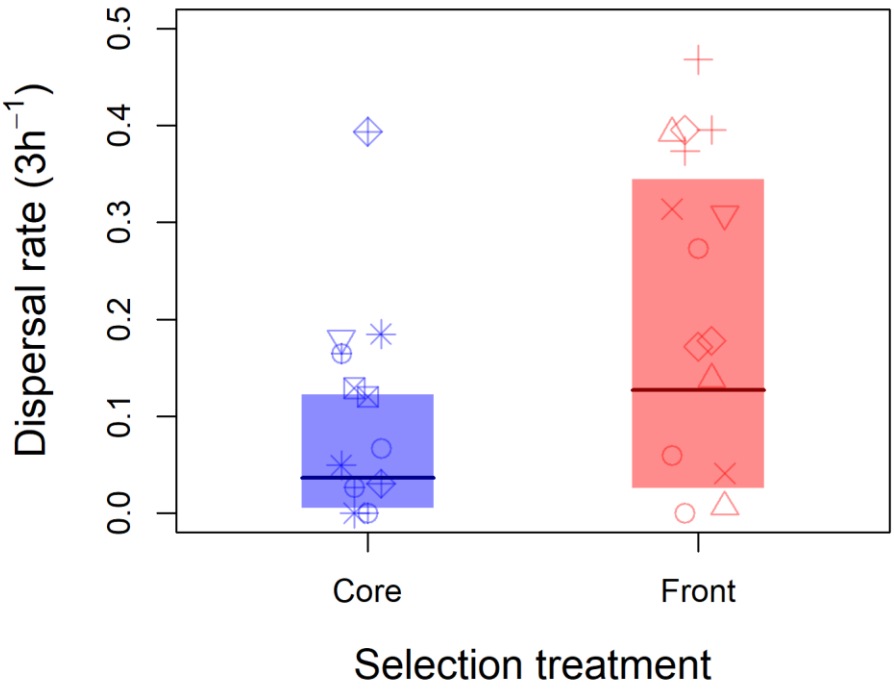

Figure 1 Dispersal rate (3 hr) of naïve unselected paramecia infected with evolved core (blue) or front (red) parasites. The solid lines represent the mean model predictions, and the shaded boxes the ±95 % CI of the model predictions. The shaded points show the mean of the selection lines for the 3 host genotypes.

Parasite life-history traits

Infectivity. Inoculation resulted in considerable levels of infection (> 50 %) for all three host genotypes (Fig. 2), but we found no significant difference in infectivity between core parasites (56 %) and front parasites (51 %; $\chi_1^2 = 0.7$, $p > 0.3$). There also were no clear patterns, when the comparison was broken down per host genotype (SI 5, Fig. S6). Differences in infection prevalence built up over the following days, when parasite development and epidemiological dynamics set in.

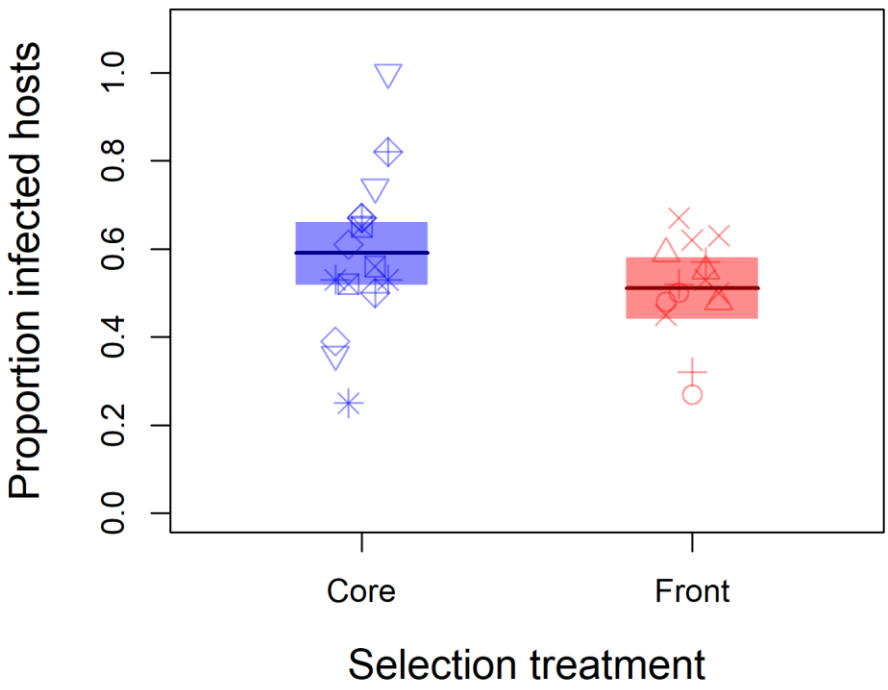

Figure 2 The proportion of infected hosts with evolved core (blue) or front (red) parasites on day 4 post infection. The solid lines represent the mean model predictions, and the shaded boxes the ±95 % CI of the model predictions. The shaded points show the mean of the selection lines for the 3 host genotypes.

Latency. The first infectious hosts appeared on day 6 p.i., and their frequency then increased over the following week, reaching up to 100% (Fig. 3). Front parasites produced a significantly lower proportion of infectious hosts than did core parasites (29% vs 37%, on average), indicating a lower rate of conversion from the reproductive to the infectious state. This tendency thus translated in a longer latency time for front parasites, meaning that the average onset of the production of horizontal transmission stages was delayed by ≈17 h relative to core parasites. Even though the decreased infectiousness of front parasites was a general

phenomenon, detailed inspection indicated that the signal of longer latency mainly comes from two of the three genotypes (SI 5, Fig. S7).

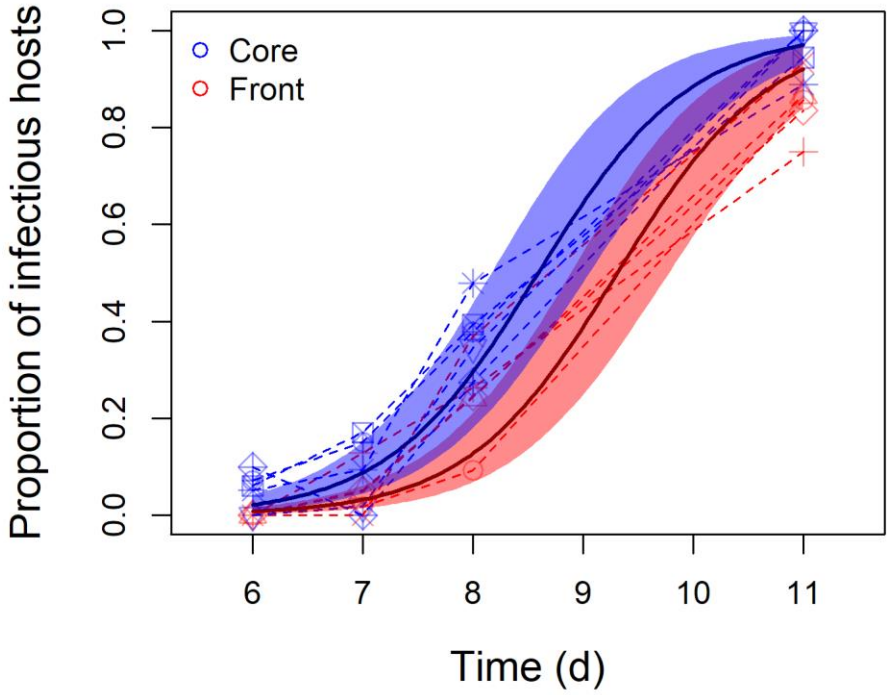

Figure 3 The proportion of infectious hosts with evolved core (blue) or front (red) parasites measure on day 6, 7, 8 and 11 post infection. The solid lines represent the mean model predictions, and the shaded curved area the ±95 % CI of the model predictions. The shaded points and dashed lines show the mean and the trajectories of the selection lines for the 3 host genotypes.

Virulence. Over the first 3 days of the assay, the majority of infected singletons (85%) went through 1-3 divisions, and in 1/3 of the cases, 1-2 additional divisions had occurred by day 10. By day 20, cell numbers had declined in all tubes (max. n = 10 individuals; Fig. 4), and extinction occurred in 70% of the tubes.

On average, hosts infected with front parasites reached 25% higher densities than those with infected with core parasites this difference was most pronounced for day 10, when density had reached a maximum (treatment x time interaction: $\chi_1^2 = 42.61$, $p < 0.0001$; Fig. 4). This general trend holds for all three host genotypes, although pronounced to different degrees (SI 5, Fig. S8).

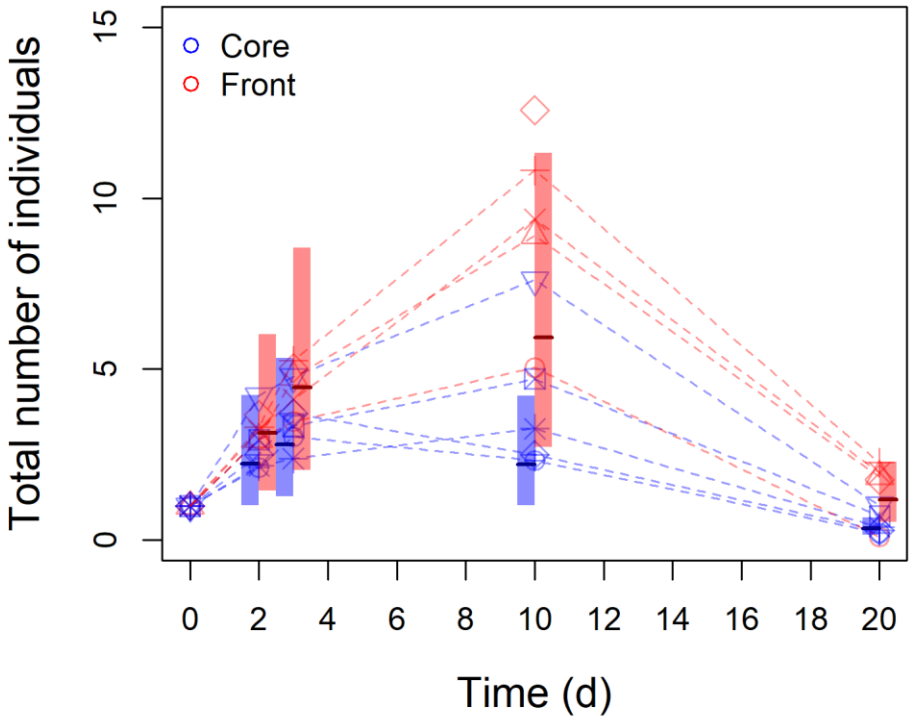

Figure 4 Total number of individuals in singleton tubes as measure for virulence. In blue and red hosts infected with evolved core or front parasites respectively. The measurements were taken on day 2, 3, 10 and 20 after isolation. The solid lines within shaded boxes represent the mean model predictions, and the shaded boxes represent the ±95 % CI of the model predictions. The shaded points and dashed lines are the mean and trajectories of the selection lines for the 3 host genotypes.

Epidemiological model fits

By fitting an epidemiological model to the population-level data from the assay replicate cultures (infection prevalence and population density), we obtained independent estimates of parasite parameters. Generally, the model succeeded in capturing the main demographic and epidemiological

dynamics observed in the cultures. This is illustrated in Fig. 5A, showing the model fits for the densities of infected and uninfected hosts for the 63D host genotype (for the other two host genotypes, see SI 6 Fig. S9). Estimates of virulence, horizontal transmission rate and latency confirm the main trends found in the above assays (Fig, 5B-D). Namely, the model fits show that front parasites have lower virulence, lower transmission rate and longer latency time than core parasites, a pattern consistent over all three host genotypes.

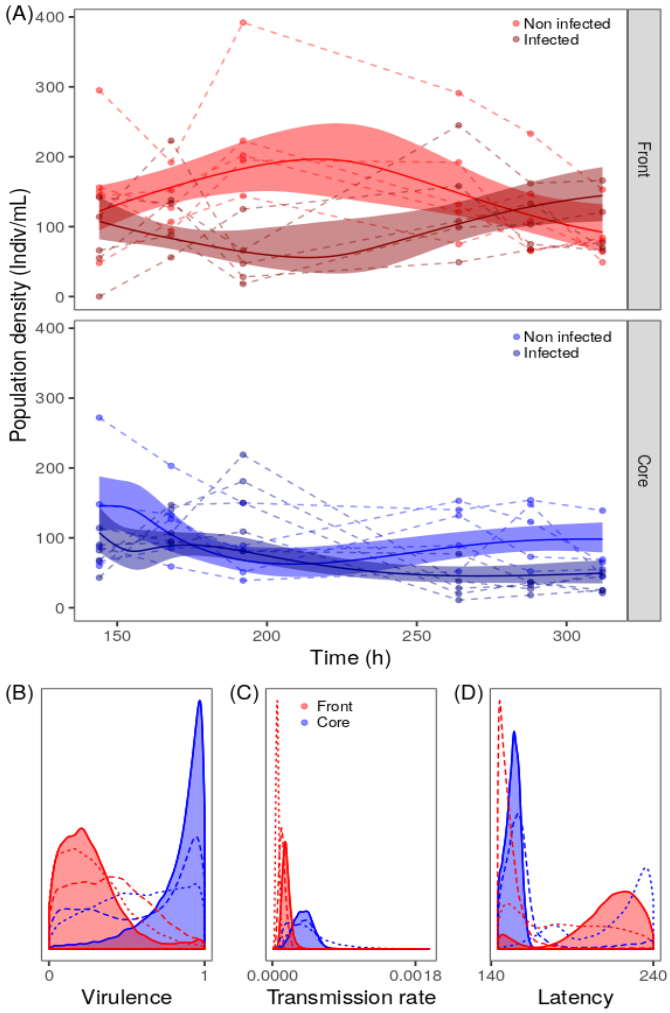

Figure 5 (A) Fit of the epidemiological model (equations 6-8) to infected and susceptible host time series data in the core and front treatment for host genotype 63D. For the two other genotypes see SI 6. Circle and dashed represent observed host population data, solid lines and shaded areas represent posterior model predictions. (B)-(D) visualize posterior distributions for virulence, transmission rate and latency respectively. The solid lines and shade areas show posteriors for genotype 63D. The dashed lines represent host clone C173, and the dotted lines host clone C023.

DISCUSSION

Consistent with empirical examples and recent theory (Osnas et al., 2015), we experimentally show that parasites develop correlated changes in several life-history traits in response to dispersal selection imposed on the host. Parasites from the front selection treatment induced higher rates of host dispersal than did parasites from the core treatment. This divergence was accompanied by lower levels of virulence and delayed development of infectious stages of front parasites. We validated these experimental results by fitting an epidemiological model to time-series data independently obtained from the experiment.

Our findings indicate the evolution of multiple traits, where selection for adaptations facilitating parasite dispersal produces concomitant changes in virulence and investment in horizontal transmission. Such rapidly evolving "invasion syndromes" have been identified in natural spreading diseases, such as avian malaria in Europe (Pérez-Tris and Bensch, 2005), or lungworms in invasive cane toads in Australia. In the latter example, lungworms at the invasion front exhibit distinct life-history traits (reduced age at maturity, larger infective and free-living larvae and larger eggs, see (Kelehear et al., 2012). We find that the evolution of such syndromes can be constrained by trade-offs between opportunities for local transmission and global dispersal. In our case, the evolution of higher dispersal at the front seemingly comes at the cost of reduced horizontal transmission potential, a trade-off resulting from a reduction in virulence. A first conclusion from this observation is that the optimal balance between transmission and host exploitation strategies depends on the way parasites disperse in space. Importantly, as we show here, dispersal itself can be the target of selection, adding another trait to the equation.

In many systems, parasites travel with their host for dispersal. Often infection reduce (Fellous et al., 2011; Nørgaard et al., 2019b, 2019a) or alter host dispersal in one way or another (Hawley et al., 2013; Thomas et al., 2002; Wesołowska and Wesołowski, 2014). The adaptive

significance of these alterations for the parasite are not always clear. With strong selection for hosts to disperse (e.g., at an invasion front), parasites either evolve adaptations to keep track with rapidly dispersing hosts or run the risk of being lost from these population altogether, which can lead to a phenomenon known as parasite release from the host perspective (Torchin *et al.* 2003). In systems where parasites disperse with their hosts such adaptations may imply a variety of solution, from prudent host exploitation to active host manipulation (Lion et al., 2006). Our experiment illustrates the capacity of parasites to evolve dispersal adaptation that can be associated with shifts in transmission strategies: parasites from the front treatment tended to invest less in horizontal transmission (Fig. 3). This result joins previous findings in this and other systems showing that transmission strategies and virulence can indeed change in response to abiotic factors or spatial structure (Jousimo *et al.*, 2014; Lion and Gandon, 2015). For example, manipulation of extrinsic mortality in the *Paramecium-Holospora* system lead to associated changes in parasite latency and virulence (Nidelet et al., 2009), similar to those observed here. Along the same lines, Magalon et al (2010) found that frequent population bottlenecking favoured less virulent parasites with a longer latency time. Their study can be re-interpreted as an extinction-recolonisation experiment, where frequent dispersal is followed by periods of low host density. This may lead to lower optimal levels of investment in horizontal transmission and virulence, and instead favour a strategy of vertical transmission (Magalon et al 2010). We prevented this latter evolutionary mechanism in the present experiment by adjusting population density in both core and front treatments after dispersal.

Population structure and opportunities for dispersal also affect experimental virulence evolution of viruses and bacteriophages (Berngruber et al., 2015; Boots and Mealor, 2007; Kerr et al., 2006). However, contrary to our results, Berngruber et al. (2015) showed that a less virulent, predominantly vertically transmitted phage outcompetes a virulent mutant in spatially structured epidemics, but goes extinct when spatial structure is eroded, i.e., under high, global

levels of dispersal (see also (Su et al., 2019). One main difference to our study is the way spatial structure and dispersal is implemented in the experiment. Berngruber et al (2015) create highly connected ‘small worlds’ by shaking experimental microcosms. This increases encounter rates with susceptible hosts and favours more transmissible parasites, thereby associating conditions of “more dispersal” with increased virulence, as predicted by theory (Kamo and Boots, 2006; Kamo et al., 2007). We obtained the opposite result of more dispersal associated with lower virulence. The main reason is that we consider a very different spatial scenario, where infected hosts actively disperse into empty space, characteristic of a biological invasion. It will be interesting to test whether we would still find lower virulence in the front selection treatment, if infected hosts disperse into patches already occupied by (susceptible) hosts. These examples illustrate how differently spatial spread and dispersal can be approached conceptually and experimentally. We argue that predictions may vary considerably depending on how parasites move through a landscape (Osnas et al., 2015; Nørgaard et al., 2019a).

In conclusion, our results show that different segments of an epidemic wave may be under divergent selection pressures. Namely, we show that parasites at an experimental invasion front are selected for traits that cause reduced virulence. This contrasts with observations of increased virulence at the front line in certain natural systems (Boots et al., 2004; Moss et al., 2002), while confirming others (Hawley et al., 2013; de Roode et al., 2008). This calls for more detailed investigations of parasite dispersal behaviour in natural populations and the consequences for parasite life-history evolution, such as virulence and transmission. Establishing a better understanding of the interaction between demography and rapid evolutionary change in spreading populations is crucial for the management of emerging diseases and disease outbreak in the wild, biological invasions and other non-equilibrium scenarios.

Acknowledgements

This work was supported by the 2019 Godfrey Hewitt mobility award granted to LN by ESEB, andby the Swiss National Science Foundation (grant no. P2NEP3_184489) to GZ.

This is publication ISEM-YYYY-XXX of the Institut des Sciences de l'Evolution -Montpellier.

Author contributions

OK, LN and GZ conceived the study. LN, GZ, CGB and OK performed the experimental work., LN, GZ, OK, MDH and EAF performed the statistical analysis. OK, EAF and CS developed, and CS analysed the model. All authors interpreted the results and contributed to writing the first draft of the manuscript. All authors commented on the final version.

Data accessibility

If the manuscript is successfully accepted for publication, data will be available at Dryad or Figshare.

REFERENCES

Andre, J.-B., and Hochberg, M.E. (2005). Virulence evolution in emerging infectious diseases. Evolution *59*, 1406–1412.

Berngruber, T.W., Froissart, R., Choisy, M., and Gandon, S. (2013). Evolution of virulence in emerging epidemics. PLoS Pathog. *9*, e1003209.

Berngruber, T.W., Lion, S., and Gandon, S. (2015). Spatial Structure, Transmission Modes and the Evolution of Viral Exploitation Strategies. PLOS Pathog. *11*, e1004810.

Boots, M., and Mealor, M. (2007). Local interactions select for lower pathogen infectivity. Science *315*, 1284–1286.

Boots, M., and Sasaki, A. (1999). "Small worlds" and the evolution of virulence: infection occurs locally and at a distance. Proc. R. Soc. B-Biol. Sci. *266*, 1933–1938.

Boots, M., Hudson, P.J., and Sasaki, A. (2004). Large shifts in pathogen virulence relate to host population structure. Science *303*, 842–844.

Brockhurst, M.A., and Koskella, B. (2013). Experimental coevolution of species interactions. Trends Ecol. Evol. *28*, 367–375.

Bull, J.J. (1994). Virulence. Evolution *48*, 1423–1437.

Calcagno, V., Mouquet, N., Jarne, P., and David, P. (2006). Coexistence in a metacommunity: the competition-colonization trade-off is not dead. Ecol. Lett. *9*, 897–907.

Dunn, A.M., and Hatcher, M.J. (2015). Parasites and biological invasions: Parallels, interactions, and control. Trends Parasitol. *31*, 189–199.

Epstein, P.R. (2000). Is global warming harmful to health? Science *283*, 50–57.

Ewald, P.W. (1995). The evolution of virulence: a unifying link between parasitology and ecology. J. Parasitol. *81*, 659–669.

Fellous, S., Quillery, E., Duncan, A.B., and Kaltz, O. (2011). Parasitic infection reduces dispersal of ciliate host. Biol. Lett. *7*, 327–329.

Fels, D., Vignon, M., and Kaltz, O. (2008). Ecological and genetic determinants of multiple infection and aggregation in a microbial host-parasite system. Parasitology *135*, 1373–1383.

Fokin, S.I., and Görtz, H.-D. (2009). Diversity of Holospora bacteria in Paramecium and their characterization. In Endosymbionts in Paramecium, pp. 162–194.

Friedenberg, N.A. (2003). Experimental evolution of dispersal in spatiotemporally variable microcosms. Ecol. 422 Lett. 6, 953–959.

Fronhofer, E.A., and Altermatt, F. (2015). Eco-evolutionary feedbacks during experimental range expansions. Nat. Commun. *6*, 6844.

Gandon, S., Mackinnon, M.J., Nee, S., and Read, A.F. (2001). Imperfect vaccines and the evolution of pathogen virulence. Nature *414*, 751–755.

Görtz, H.D., and Dieckmann, J. (1980). Life cycle and infectivity of Holospora elegans Haffkine, a micronucleus-specific symbiont of Paramecium caudatum (Ehrenberg). Protistologia *16*, 591–603.

Griette, Q., Raoul, G., and Gandon, S. (2015). Virulence evolution at the front line of spreading epidemics. Evolution *69*, 2810–2819.

Hawley, D.M., Osnas, E.E., Dobson, A.P., Hochachka, W.M., and Ley, D.H. (2013). Parallel patterns of increased virulence in a recently emerged wildlife pathogen. PLoS Biol. *11*.

Jousimo, J., Tack, A.J.M., Ovaskainen, O., Mononen, T., Susi, H., Tollenaere, C., and Laine, A.-L. (2014). Ecological and evolutionary effects of fragmentation on infectious disease dynamics. Science *344*, 1289–1293.

Kamo, M., and Boots, M. (2006). The evolution of parasite dispersal, transmission, and virulence in spatial host populations. Evol. Ecol. Res. *8*, 1333–1347.

Kamo, M., Sasaki, A., and Boots, M. (2007). The role of trade-off shapes in the evolution of parasites in spatial host populations: An approximate analytical approach. J. Theor. Biol. *244*, 588–596.

Kelehear, C., Brown, G.P., and Shine, R. (2012). Rapid evolution of parasite life history traits on an expanding range-edge. Ecol. Lett. *15*, 329–337.

Kerr, B., Neuhauser, C., Bohannan, B.J.M., and Dean, A.M. (2006). Local migration promotes competitive restraint in a host–pathogen "tragedy of the commons." Nature *442*, 75–78.

Lion, S., and Gandon, S. (2015). Evolution of spatially structured host-parasite interactions. J. Evol. Biol. *28*, 10–28.

Lion, S., van Baalen, M., and Wilson, W.G. (2006). The evolution of parasite manipulation of host dispersal. Proc. R. Soc. B Biol. Sci. *273*, 1063–1071.

Magalon, H., Nidelet, T., Martin, G., and Kaltz, O. (2010). Host growth conditions influence experimental evolution of life history and virulence of a parasite with vertical and horizontal transmission. Evolution *64*, 2126–2138.

May, R.M., and Anderson, R.M. (1983). Epidemiology and genetics in the coevolution of parasites and hosts. Proc. R. Soc. Lond. - B Biol. Sci. *219*, 281–313.

Mondet, F., de Miranda, J.R., Kretzschmar, A., Le Conte, Y., and Mercer, A.R. (2014). On the front line: Quantitative virus dynamics in honeybee (Apis mellifera L.) colonies along a new expansion front of the parasite Varroa destructor. PLoS Pathog. *10*, e1004323.

Moss, S.R., Turner, S.L., Trout, R.C., White, P.J., Hudson, P.J., Desai, A., Armesto, M., Forrester, N.L., and Gould, E.A. (2002). Molecular epidemiology of rabbit haemorrhagic disease virus. J. Gen. Virol. *83*, 2461–2467.

Nidelet, T., and Kaltz, O. (2007). Direct and correlated responses to selection in a host-parasite system: Testing for the emergence of genotype specificity. Evolution *61*, 1803–1811.

Nidelet, T., Koella, J.C., and Kaltz, O. (2009). Effects of shortened host life span on the evolution of parasite life history and virulence in a microbial host-parasite system. BMC Evol. Biol. *9*, 1–10.

Nørgaard, L.S., Phillips, B.L., and Hall, M.D. (2019a). Infection in patchy populations: Contrasting pathogen invasion success and dispersal at varying times since host colonization. Evol. Lett. *3*, 555–566.

Nørgaard, L.S., Phillips, B.L., and Hall, M.D. (2019b). Can pathogens optimize both transmission and dispersal by exploiting sexual dimorphism in their hosts? Biol. Lett. *15*, 20190180.

Olivieri, I., Michalakis, Y. & Gouyon, P.-H. (1995). Metapopulation genetics and the evolution of dispersal. Am. Nat., 146, 202-228.

Osnas, E.E., Hurtado, P.J., and Dobson, A.P. (2015). Evolution of pathogen virulence across space during an epidemic. Am. Nat. *185*, 332–342.

Parratt, S.R., Numminen, E., and Laine, A.-L. (2016). Infectious disease dynamics in heterogeneous landscapes. Annu. Rev. Ecol. Evol. Syst. *47*, 283–306.

Penczykowski, R.M., Laine, A.L., and Koskella, B. (2016). Understanding the ecology and evolution of host-parasite interactions across scales. Evol. Appl. *9*, 37–52.

Pérez-Tris, J., and Bensch, S. (2005). Dispersal increases local transmission of avian malarial parasites. Ecol. Lett. *8*, 838–845.

Perkins, A.A., Phillips, B.L., Baskett, M.L., and Hastings, A. (2013). Evolution of dispersal and life history interact to drive accelerating spread of an invasive species. Ecol. Lett. *16*, 1079–1087.

Perkins, S.E., Altizer, S., Bjornstad, O., Burdon, J.J., Clay, K., Gómez-aparicio, L., Jeschke, J.M., Johnson, P.T.J., LAFFERTY, Kevin, D., Malmstrom, C.M., et al. (2008). Invasion Biology and Parasitic Infections. In Infectious Disease Ecology, p.

Phillips, B.L., and Puschendorf, R. (2013). Do pathogens become more virulent as they spread? Evidence from the amphibian declines in Central America. Proc. Biol. Sci. *280*, 20131290.

Phillips, B.L., Brown, G.P., and Shine, R. (2010). Evolutionarily accelerated invasions: The rate of dispersal evolves upwards during the range advance of cane toads. J. Evol. Biol. *23*, 2595–2601.

Restif, O., and Kaltz, O. (2006). Condition-dependent virulence in a horizontally and vertically transmitted bacterial parasite. Oikos *114*, 148–158.

de Roode, J.C., Yates, A.J., and Altizer, S. (2008). Virulence-transmission trade-offs and population divergence in virulence in a naturally occurring butterfly parasite. Proc. Natl. Acad. Sci. *105*, 7489–7494.

Rosenbaum, B., Raatz, M., Weithoff, G., Fussmann, G.F., and Gaedke, U. (2019). Estimating Parameters from Multiple Time Series of Population Dynamics Using Bayesian Inference. Front. Ecol. Evol. *6*.

Su, M., Chen, G., and Yang, Y. (2019). Dynamics of host-parasite interactions with horizontal and vertical transmissions in spatially heterogeneous environment. Phys. Stat. Mech. Its Appl. *517*, 452–458.

Thieme, H. R. (2018). Mathematics in population biology (Vol. 12). Princeton University Press.

Thomas, D.D. (2000). Dispersal and extinction in fragmented landscapes. Proc. Biol. Sci. - R. Soc. *267*, 139–145.

Thomas, F., Schmidt-Rhaesa, A., Martin, G., Manu, C., Durand, P., and Renaud, F. (2002). Do hairworms (Nematomorpha) manipulate the water seeking behaviour of their terrestrial hosts? J. Evol. Biol. *15*, 356–361.

Torchin, M.E., Lafferty, K.D., Dobson, A.P., McKenzie, V.J., and Kuris, A.M. (2003). Introduced species and their missing parasites. Nature *421*, 628–630.

Vogwill, T., Fenton, A. & Brockhurst, M.A. (2010). How does spatial dispersal network affect the evolution of parasite local adaptation? Evolution, 64, 1795-1801

Wesołowska, W., and Wesołowski, T. (2014). Do Leucochloridium sporocysts manipulate the behaviour of their snail hosts? J. Zool. *292*, 151–155.

Wichterman, R. (1986). The biology of Paramecium (Plenum Press, New York).

Williams, J.L., Kendall, B.E., and Levine, J.M. (2016). Rapid evolution accelerates plant population spread in 528 fragmented experimental landscapes. Science 353, 482–485.

Zilio, G., Noergaard, L.S., Gougat-Barbera, C., Hall, M.D., Fronhofer, E.A., and Kaltz, O. (2020). Travelling with a parasite: the evolution of resistance and dispersal syndrome during experimental range expansion. BioRxiv 2020.01.29.924498.

SUPPLEMENTARY INFORMATION

SI 1 Selection protocol

The experimental system consisted of two 14 mL plastic tubes (the core and front patch, Fig. S1) interconnected by a 5 cm silicon tube of 0.6 mm inner diameter (corridor). We first filled the two-patch system with 9.5 mL of fresh growth medium and we then closed the corridor with a clamp. Secondly, we filled to 13 mL one of the two tubes, the core patch, using the paramecia and medium from an experimental selection line. The second tube, the front patch, was filled to 13 mL with fresh growth medium, and thus resulted empty at this stage. Thirdly, we removed the clamp and opened the corridor allowing the paramecia to actively disperse and swim from core to front patch or to stay in the core. After three hours, we closed the corridor tube and we estimated the population density by taking a 200 µL sample from core and front patch and counting the number of individuals under a dissecting microscope. Each line was then cultured for a further week in 20 mL of bacterised lettuce medium, before the next dispersal and selection event occurred.

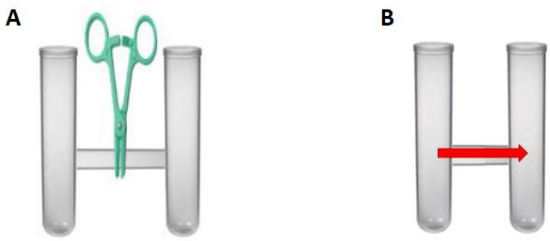

Figure S1. A) Experimental two-patch system with corridor for the selection protocol composed by a core and front patch, left and right tube respectively. B) The opening of the clamp allows the hosts to actively disperse from the left to the right through the connecting tube (from core to front).

For the first 30 dispersal/growth cycles, we adjusted *Paramecium* densities between treatments for the initial number of individuals placed in the core patch before the dispersal event (~2000 individuals), and for the number of *Paramecium* transferred after dispersal (~200 individuals).

After cycle 30, we extracted infectious forms from each selection line, inoculated a new 63D hosts, and continued the selection experiment for another 26 cycles with a relaxed density adjustment protocol. During these last 26 cycles, we ceased correcting for density at each dispersal episode to allow to for more natural range expansion growth dynamics to occur. The experimental design of the selection protocol is described in the main text and illustrated in Fig. S2.

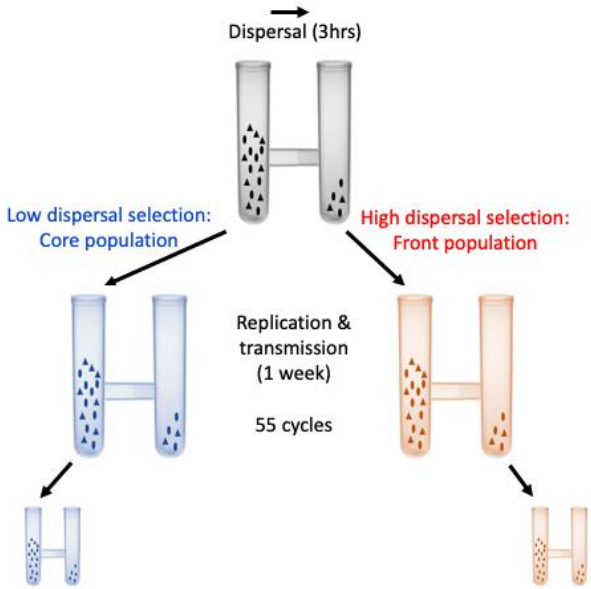

Figure S2. Experimental evolution setup. We selected for high (red) and low (blue) dispersal by weekly allowing for active dispersal of coevolving host and parasites in two-patch microcosms during a three-hour period. At each cycle, dispersing (infected and uninfected) individuals were transferred to a new tube, representing the high selection treatment, whereas residing individuals is transferred to another tube representing the low dispersal selection treatment. This procedure was repeated for 55 cycles after which we isolated the evolved parasites to test for evolutionary adaptations.

SI 2 Extraction protocol

Infected paramecia were transferred in Falcon tubes filled with 15 mL of medium. These were centrifuged at 3500 RPM for 20 minutes. The supernatant was removed, and the concentrated individuals were transferred into 1.5 mL Eppendorf tubes containing 1 mm glass beads. Using a Qiagen TissuLyser they were then vortexed and crushed (1.45 minutes at 30 oscillation

frequency). The infectious forms were then counted at 200 x magnification under a microscope (Leica DM LB2), using a hemocytometer. The final inocula for the infections were obtained by adjusting the concentration with sterile water.

SI 3 Long-term experiment: trajectories

Routine measurements taken during the long-term experiment indicate differences between the core and front selection treatments for dispersal and demography. Over the first 30 cycles, and then again after resetting the evolving parasites on new naive hosts (cycle 31-55), infected populations in the front selection treatment showed up to three times higher dispersal rates than core populations (46 out of 53 treatment cycle means; Fig. S3A). Front populations also reached on average 1.5x higher population densities than core populations (45 out of 53 means; Fig. S3B). To separate parasite from host responses to the applied dispersal selection treatments, the following assays tested evolved parasites on three genotypes of naïve hosts after 55 cycles of experimental selection for high (front) and low (core) dispersal.

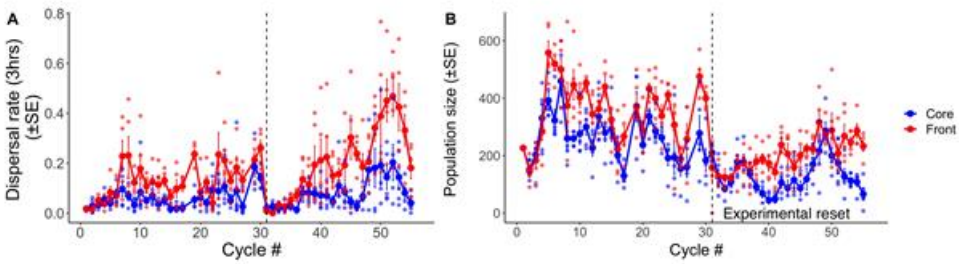

Figure S3. Long-term experimental selection data for A) dispersal rate and B) population size. Red dots represent populations (host and parasite) selected for high dispersal (front population), and blue represent populations selected for low dispersal (core population). Filled, large dots and connecting lines are mean values across selection lines (±SE), and dull small points represent raw data from individual selection lines at each dispersal cycle. Grey dashed line indicates the experimental reset at cycle 31, when evolved parasites were extracted and re-inoculated on naive hosts.

SI 4 Assay details

Infectivity

Inocula of the evolved parasites selected for high or low dispersal (front and core, respectively) were obtained following the aforementioned extraction protocol. These were used to infect unselected naïve host populations of three genotypes: 63D, C023 and C173. The number of infectious forms obtained from individual selection lines varied up to one order of magnitude, but all inoculation doses were higher than previously applied infection doses in this system. Below a threshold of ~10-20 infective forms per µL, there is no evidence of dose dependency in this system. Our inocula doses ranged from ~35 to ~1000 infective spores per µL (comparable dose in this system) and we would therefore expect maximum infection success for all selection lines. Preliminary logistic regression with binomial error structure (logit link) was used to screen for inocula dose effects on infection success, but revealed no significant effect ($\chi_7^2 = 10.812$, $p = 0.147$). Thus, we found no evidence for correcting infection success for inocula dose in this system, indicating that all inoculations had reached maximum infection capacity at the applied dose. Lastly, infections are usually confounded by one to 3 infectious forms that are up taken by filter feeding, and infection occur within 24 hrs post inoculation.

Dispersal assay

In order to obtain higher numbers of dispersers, we implemented the dispersal 2-patch system used for the selection protocol (see above). We assayed dispersal in linear 3-patch arenas (50 mL Falcon tubes; Fig. S4), which allowed us to use bigger volumes of culture. *Paramecium* dispersed from the middle tube into the two outer tubes. To further increase the resolution of dispersal estimates, we concentrated the cultures 12 h prior to the assay, by gentle centrifugation at 1200 RPM for 15 minutes. Briefly, we first filled the 3-patch system with 20 mL of fresh growth medium, and we then closed the two corridors with clamps. Second, we

added to the middle tube ~2800 individuals and we filled it to 25 mL adding fresh growth medium. Third, the outer tubes were filled to 25 mL, clamps were removed and the connections were opened for 3 h, dispersal rates and densities were then estimated by counting the Paramecium in samples from the central tube (500 µl) and from the combined two outer tubes (3 mL). From these estimates we calculated the dispersal rate of infected hosts. In total, 99 dispersal assays were conducted (90 infected populations and 9 uninfected mock cultures across the three host genotypes), with at least one replicate of each treatment combination tested per day. For statistical analysis, we excluded 16 replicates with very low population density and/or infection prevalence (<10%), which prevented accurate estimation of dispersal of infected individuals.

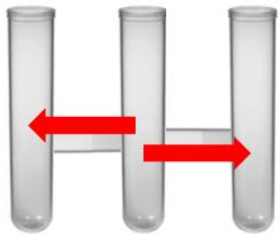

Figure S4. Linear 3-patch arenas used for the dispersal assays. *Paramecium* was added in the central tube and after the opening of the connections it was allowed to disperse (3h) in the outer tube as indicated by the red arrows.

SI 5 Results

Dispersal

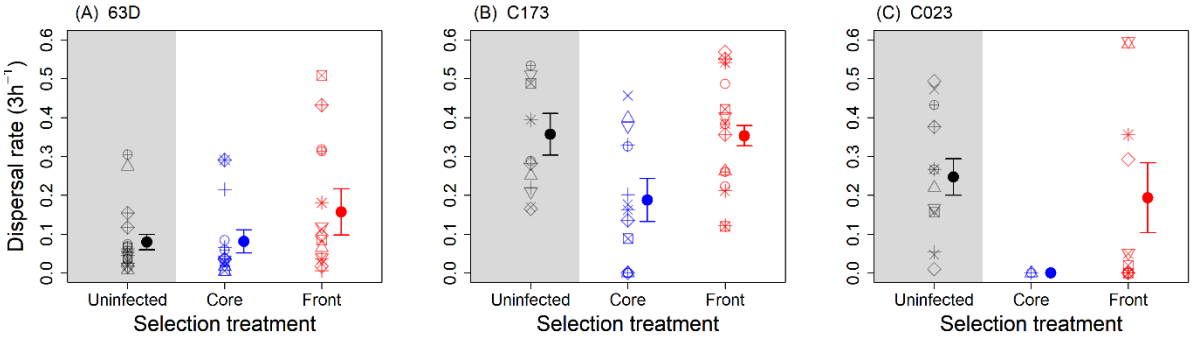

Figure S5. Mean dispersal rate (3 hr) of naïve unselected paramecia infected with evolved core (blue) or front (red) parasites and the reference uninfected culture (black). Shown in full dots are the overall means (±SE) for the 3 host genotypes. Empty dots represent raw data for individual selection line and 3 graphs represent the three naïve host genotypes.

Infectivity

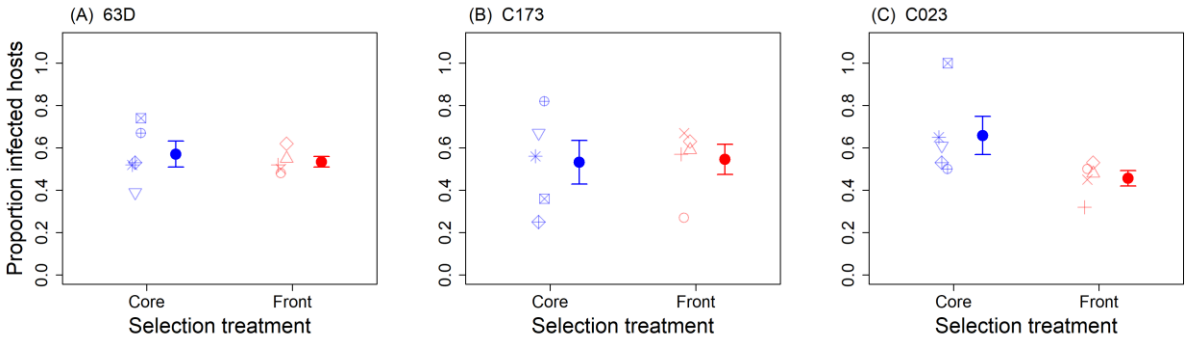

Figure S6. Proportion of infected individuals in populations inoculated with evolved core (blue) or front (red) parasites on day 4 post infection for the 3 host genotypes (3 graphs). Full dots are the overall means (±SE) and empty dots the mean of the selection lines. Note that these data were obtained before to split multiply each selection line in the technical replicates.

Latency

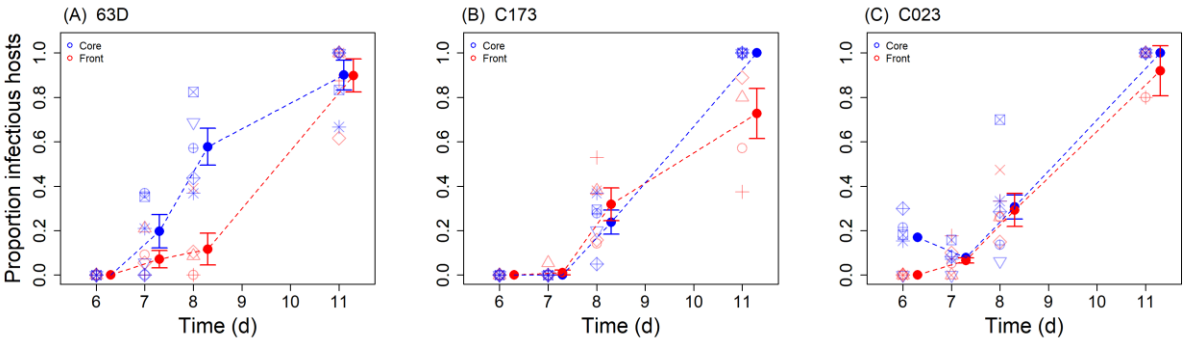

Figure S7. Proportion of infectious hosts (host carrying infectious spores) on day 6, 7, 8 and 11 post infection, each graph corresponds to a host genotype. The full dots, blue for the core and red for the front treatment, are the overall mean for each day (±SE) connected by dashed lines. The shaded dots are the mean of the selection lines on the 4 different days of inspection.

Virulence

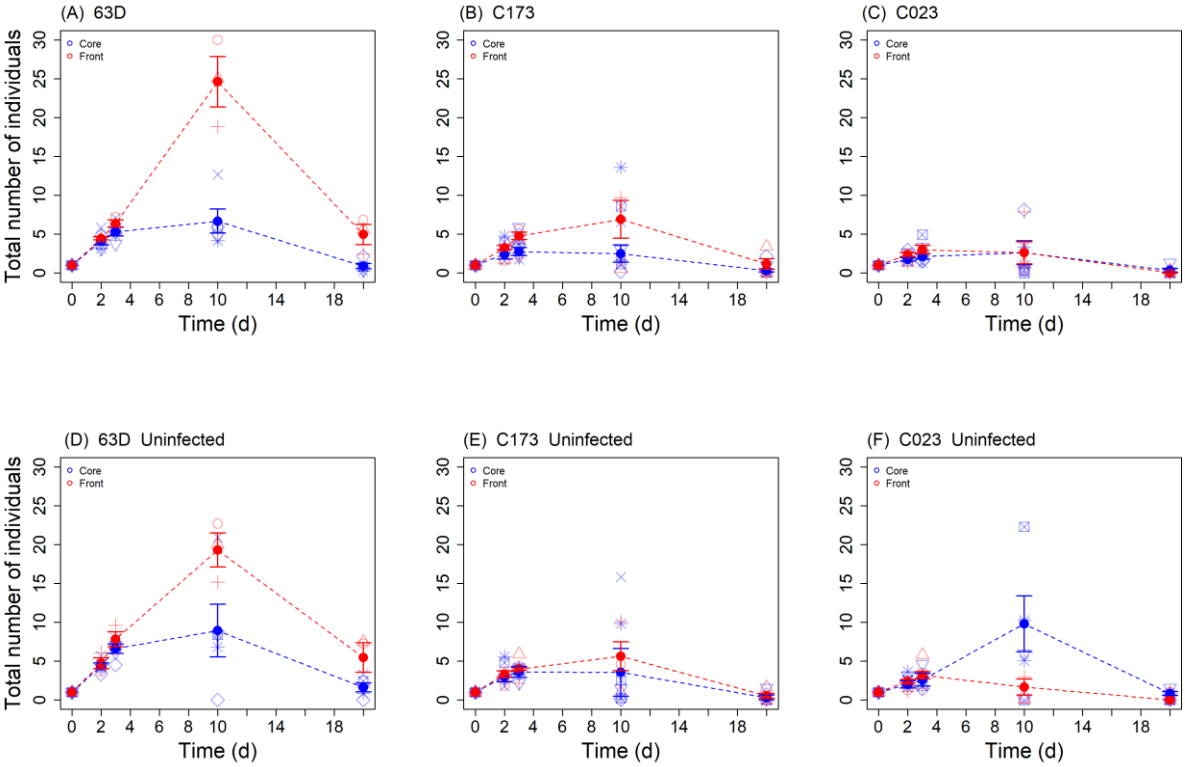

Figure S8. Total number of infected (top row A, B, C) and uninfected (bottom row D, E, F) individuals counted on day 2, 4, 10 and 20 post isolation in singleton tubes for the 3 host genotypes. The full dots, blue for the core and red for the front treatment, are the overall mean for each day (±SE) connected by dashed lines. The shaded dots are the mean of the selection lines.

SI 6 Epidemiological model fits

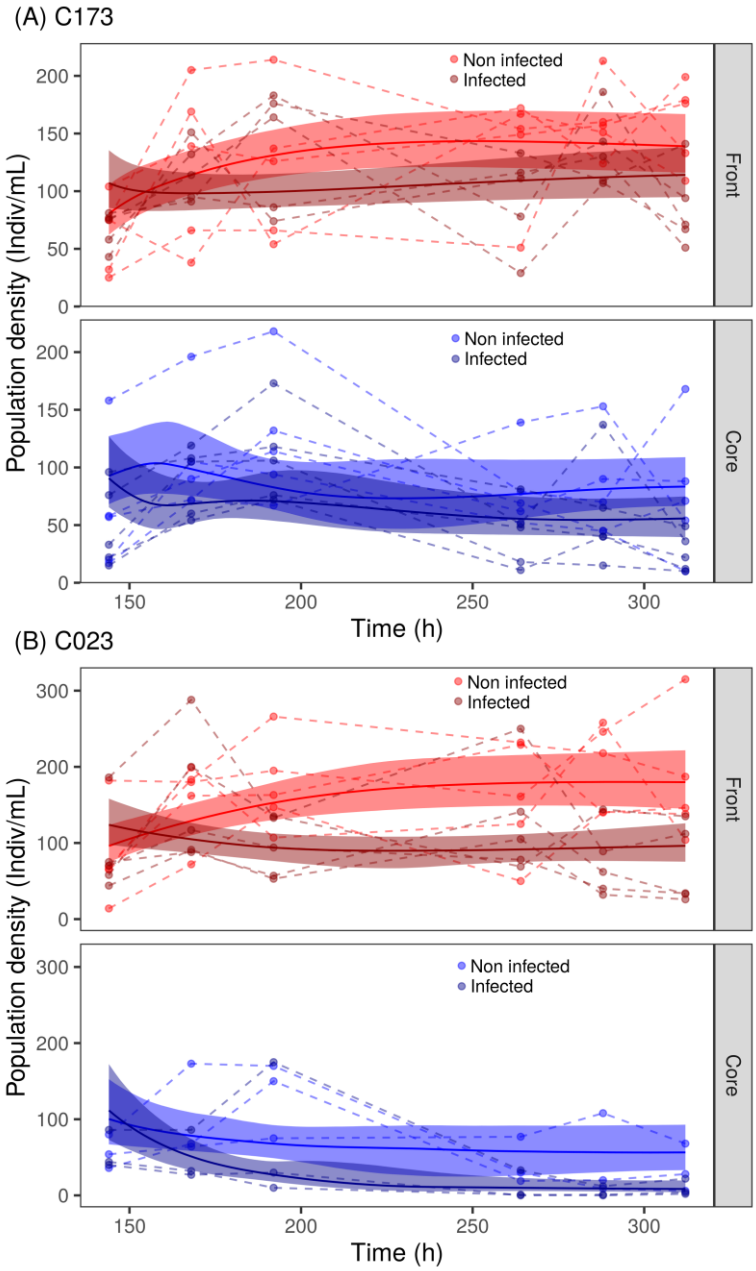

Figure S9 Fit of the epidemiological model (equations 6-8) to infected and susceptible host time series data in the core and front treatment for host genotype (A) C173 and (B) C023. Circle and dashed represent observed host population data, solid lines and shaded areas represent posterior model predictions.